Molecular Human Reproduction, pp. 1–15, 2021
https://doi.org/10.1093/molehr/gaab066

molecular human reproduction

ORIGINAL RESEARCH

Dissecting EPPIN protease inhibitor domains in sperm motility and fertilizing ability: repercussions for male contraceptive development

Alan A.S. Silva[1,†], Tamiris R.F. Raimundo[1,†], Noemia A.P. Mariani[1], Hélio Kushima[1], Maria Christina W. Avellar[2], Mariano G. Buffone[3], Fabíola F. Paula-Lopes[4], Marcelo T. Moura[4], and Erick J.R. Silva[1,*]

[1]Department of Biophysics and Pharmacology, Institute of Biosciences, São Paulo State University, Botucatu-SP, Brazil [2]Department of Pharmacology, Universidade Federal de São Paulo–Escola Paulista de Medicina, São Paulo-SP, Brazil [3]Instituto de Biología y Medicina Experimental, Consejo Nacional de Investigaciones Científicas y Técnicas, Buenos Aires, Argentina and [4]Department of Biological Sciences, Universidade Federal de São Paulo—Campus Diadema, Diadema-SP, Brazil

Correspondence address. Department of Biophysics and Pharmacology, Institute of Biosciences, São Paulo State University, Rua Prof. Dr. Antonio Celso W. Zanin, S/N, Botucatu-SP, 18618-689, Brazil. E-mail: ejr.silva@unesp.br https://orcid.org/0000-0002-9330-8658

Submitted on September 14, 2021; resubmitted on October 28, 2021; editorial decision on November 12, 2021

ABSTRACT: EPPIN (epididymal protease inhibitor) is a mammalian conserved sperm-binding protein displaying an N-terminal WFDC (whey-acidic protein four-disulfide core) and a C-terminal Kunitz protease inhibitor domains. EPPIN plays a key role in regulating sperm motility after ejaculation via interaction with the seminal plasma protein SEMG1 (semenogelin-1). EPPIN ligands targeting the SEMG1 binding site in the Kunitz domain are under development as male contraceptive drugs. Nevertheless, the relative contributions of EPPIN WFDC and Kunitz domains to sperm function remain obscure. Here, we evaluated the effects of antibodies targeting specific epitopes in EPPIN's WFDC (Q20E antibody, Gln20-Glu39 epitope) and Kunitz (S21C and F21C antibodies, Ser103-Cys123 and Phe90-C110 epitopes, respectively) domains on mouse sperm motility and fertilizing ability. Computer-assisted sperm analysis showed that sperm co-incubation with S21C antibody (but not F21C antibody) lowered progressive and hyperactivated motilities and impaired kinematic parameters describing progressive (straight-line velocity; VSL, average path velocity; VAP and straightness; STR) and vigorous sperm movements (curvilinear velocity; VCL, amplitude of lateral head movement; ALH, and linearity; LIN) compared with control. Conversely, Q20E antibody-induced milder inhibition of progressive motility and kinematic parameters (VAP, VCL and ALH). Sperm co-incubation with S21C or Q20E antibodies affected *in vitro* fertilization as revealed by reduced cleavage rates, albeit without changes in capacitation-induced tyrosine phosphorylation. In conclusion, we show that targeting specific epitopes in EPPIN Kunitz and WFDC domains inhibits sperm motility and capacitation-associated events, which decrease their fertilizing ability; nevertheless, similar observations *in vivo* remain to be demonstrated. Simultaneously targeting residues in S21C and Q20E epitopes is a promising approach for the rational design of EPPIN-based ligands with spermostatic activity.

Key words: male contraception / spermatozoon / sperm motility / hyperactivation / capacitation / fertilization / drug target

Introduction

Despite the availability of different modern contraceptive methods, almost 40% of pregnancies are unintended worldwide (Sedgh *et al.*, 2014). These alarmingly high pregnancy rates put at risk the lives and well-being of millions of women annually and are associated with negative socio-economic outcomes for them and their families (Tsui *et al.*, 2010). Innovations in contraception can prevent up to 15% of maternal deaths due to abortion or pregnancy-related issues (Tsui *et al.*, 2010; Gossett *et al.*, 2013). In this scenario, novel male contraceptives are urgently needed, given that (i) male options are limited to condoms, which have high typical failure rates, or vasectomy, which requires a medical procedure and is not readily reversible; and (ii) one in three couples rely on

†The authors consider that the first two authors should be regarded as joint First Authors.

male contraceptive methods as their main contraceptive choice (Amory, 2016). Moreover, the development of a 'male pill' remains crucial to fostering gender equality in carrying the contraceptive burden.

Sperm-binding proteins with essential roles in sperm function are promising targets for non-hormonal, fast-onset and loss-of-function male contraceptive drug development. Owing to its druggable properties and crucial roles in regulating sperm motility, the cysteine-rich protein epididymal protease inhibitor (EPPIN) is a compelling sperm target for male contraception in humans (O'Rand et al., 2016; Drevet, 2018; Long et al., 2019). EPPIN contains two protease inhibitor-type domains in its primary sequence: a whey-acidic protein four-disulfide core (WFDC) domain in the N-terminal region and a Kunitz domain in the C-terminal region.

EPPIN expression in mammals (e.g., humans and mice) is enriched in the testis and epididymis (Richardson et al., 2001; Sivashanmugam et al., 2003; Mariani et al., 2020; Robertson et al., 2020). EPPIN is found in the head and flagellum of mature spermatozoa, where it acts as a central node for protein-protein interactions that regulate sperm function upon ejaculation (Wang et al., 2005, 2007a,b; Mariani et al., 2020). EPPIN binds to the semen coagulum protein semenogelin-1 (SEMG1) in human spermatozoa, yielding a temporary loss of sperm progressive motility upon ejaculation (Wang et al., 2005; Mitra et al., 2010; Silva et al., 2013). Similarly, EPPIN is a docking site for the seminal vesicle-secreted protein 2 (SVS2), a SEMG1 orthologue, in mouse spermatozoa, supporting the hypothesis that the roles of EPPIN in sperm function are conserved between humans and mice (Mariani et al., 2020). Human and mouse EPPIN are highly conserved in their primary structure, reaching ~80% identity in their WFDC and Kunitz domain sequences (Clauss et al., 2005). Moreover, human SEMG1 and mouse SVS2 display similar roles as inhibitors of sperm capacitation-associated events such as hyperactivation and acrosomal exocytosis and promote sperm survival in the uterus (de Lamirande et al., 2001, 2010; de Lamirande, 2007; Kawano and Yoshida, 2007; Sakaguchi et al., 2020). These results indicate that EPPIN binding is a crucial event for the modulation of sperm function by SEMG1 and SVS2 alike. Single nucleotide polymorphisms in the human *EPPIN* gene have been associated with both decreased and increased risk of idiopathic infertility in men with poor semen parameters (Ding et al., 2010a,b).

Active immunization of male monkeys with recombinant human EPPIN results in high anti-EPPIN antibody titers and leads to reversible male infertility, which has triggered its development as a contraceptive drug target (O'Rand et al., 2004). Further studies showed that spermostatic anti-EPPIN antibodies and SEMG1 possess overlapping binding sites in the EPPIN Kunitz domain (O'Rand et al., 2011, 2016; Silva et al., 2012a). This knowledge facilitated the design of experimental small organic ligands targeting the EPPIN Kunitz domain, such as the lead compound EP055, which showed inhibitory sperm motility activity in human and non-human primate models (O'Rand et al., 2018). However, bioinformatic studies on full-length human EPPIN homology models indicate that amino acid residues in the EPPIN WFDC domain can also be involved in SEMG1 and EP055 binding and form intramolecular bonds with residues in the Kunitz domain that stabilize EPPIN structure (Shan et al., 2019). These findings are in agreement with observations that both EPPIN WFDC and Kunitz domains play differential roles in EPPIN functions. For instance, the EPPIN Kunitz domain, but not its WFDC domain, inhibits neutrophil elastase and serine protease prostate-specific antigen (Wang et al., 2007a,b; McCrudden et al., 2008), whereas both domains contribute to its antimicrobial activity (Yenugu et al., 2004; McCrudden et al., 2008).

Nevertheless, the relative contributions of EPPIN WFDC and Kunitz domains to the regulation of sperm function are yet to be determined. Here, we report that anti-EPPIN antibodies mapping to epitopes in EPPIN WFDC domain (Q20E antibody, which maps EPPIN Gln20-Glu39 sequence) and Kunitz domain (S21C and F21C antibodies, which map EPPIN Phe90-Cys110 and Ser103-Cys123 sequences, respectively) differentially impair motility, fertilization and capacitation-associated parameters in mouse spermatozoa. Our results demonstrate that both the Kunitz and WFDC EPPIN domains play roles in the fertilizing capacity of spermatozoa via disturbances in motility and capacitation-associated events. Our study sheds new light on the roles played by EPPIN domains in regulating sperm function, thus contributing to the concept of its development as a male contraceptive drug target with clinical applications.

Materials and methods

Reagents and chemicals

Reagents were molecular biology grade purchased from Sigma-Aldrich (St Louis, MO, USA) or Thermo Fisher Scientific (Waltham, MA, USA). HTF (human tubal fluid, 90125) medium was purchased from Irvine Scientific (Santa Ana, CA, USA). KSOMaa medium (MR106-D) was purchased from Merck (Darmstadt, Germany). Secondary antibodies were purchased from Jackson ImmunoResearch Laboratories, Inc. (West Grove, PA, USA).

Animals

We used C57BL/6 male mice (90–120 days old), purchased from Anilab Laboratory (Paulínia, SP, Brazil). For IVF, we used male Swiss mice (90–120 days old) and hybrid F1 female breed from male Balb/c and female C57BL/6 mice (CB6F1, 60–90 days old). Animals were housed under controlled conditions (12 h light/dark cycle, 22–24°C), with food and water *ad libitum*. We performed all animal experiments in compliance with the Animal Research: Reporting of *In Vivo* Experiments guidelines, the Guide for the Care and Use of Laboratory Animals (National Institutes of Health, USA) and the National Council of Animal Experimentation (CONCEA, Brazil) guidelines for animal care and use of laboratory animals. Animal procedures were approved by the Research Committee in the Use of Animals from IBB/UNESP (processes #1049 and #1138) and UNIFESP-Diadema (process #2521131119).

Anti-EPPIN antibodies

Affinity-purified rabbit polyclonal anti-EPPIN antibodies mapping N- and C-terminal sequences of EPPIN were used in our analyses (Table I). Anti-EPPIN S21C and F21C antibodies to the C-terminal of human EPPIN were kindly provided by Dr Michael G. O'Rand, the University of North Carolina at Chapel Hill (UNC-CH), USA. Anti-EPPIN Q20E polyclonal antibody to the N-terminal of murine EPPIN was produced by GenScript Inc. (Piscataway, NJ, USA). We confirmed the specificity of all anti-EPPIN antibodies in positive control

Table I Information about antibodies used in our experiments.

Anti-EPPIN antibody	Epitope sequence	Region/domain	NCBI accession number[a]
S21C	^{103}SMFVYGGCQGNNNNFQSKANC^{123}	C-terminal/Kunitz	NP_065131
F21C	^{90}FLHWWYDKKDNTCSMFVYGGC^{110}	C-terminal/Kunitz	NP_065131
Q20E	^{20}QGPSLADLLFPRRCPRFREE^{39}	N-terminal/WFDC	NP_083601

[a] NCBI (National Center for Biotechnology Information; https://www.ncbi.nlm.nih.gov/).

experiments by using recombinant GST-tagged full-length mouse EPPIN (Supplementary Fig. S1). Moreover, all antibodies detected the same immunoreactive bands corresponding to EPPIN in mouse epididymal spermatozoa total protein extracts (Supplementary Fig. S1). S21C and Q20E Fab fragments were produced by incubating the whole antibodies with papain by using standard protocols (RheaBiotech, Campinas, SP, Brazil). We dialyzed anti-EPPIN antibodies against sperm culture media before all experiments.

Isolation of mouse epididymal spermatozoa

We collected spermatozoa from mouse caput (including the initial segment), corpus and cauda epididymidis. We killed the animals by cervical dislocation and dissected their epididymides in pre-warmed sterile saline solution (0.9% w/v NaCl). We transferred epididymal regions to 12-well culture plates containing pre-warmed HTF or TYH (Toyoda, Yokoyama and Hoshi; 100 mM NaCl, 4.7 mM KCl, 1.2 mM KH_2PO_4, 1.2 mM $MgSO_4$, 5.5 mM glucose, 0.8 mM pyruvic acid, 1.7 mM $CaCl_2$ and 20 mM HEPES, pH 7.2–7.4) medium. Each epididymal region was cut with scissors and incubated at 37 °C for 10 min in a controlled atmosphere (5%/95% CO_2/air) to release spermatozoa to the medium. Next, we removed the tissues from the plate well and then counted spermatozoa in a Neubauer chamber. For sperm capacitation, we incubated cauda epididymal spermatozoa in TYH medium supplemented with 25 mM $NaHCO_3$ and 0.75% w/v bovine serum albumin (BSA; fat-free and IgG-free) for 2 h at 37 °C and 5%/95% CO_2/air. Spermatozoa were immediately processed for western blotting, immunofluorescence and functional analyses as described below.

Preparation of sperm-soluble and -insoluble protein fractions

Triton X-100-soluble and -insoluble sperm protein fractions were obtained as previously described (Visconti *et al.*, 1996), with minor modifications. Briefly, we centrifuged aliquots of sperm suspension from each epididymal region (1.5–5.0 × 10^6 cells) at 800*g* (5 min) and washed the cell pellet with phosphate buffer (100 mM sodium phosphate, 150 mM NaCl, pH 7.2). Spermatozoa were resuspended in TET buffer (1% v/v Triton X-100, 50 mM Tris-HCl, 1 mM EDTA, pH 7.5) containing protease inhibitor cocktail (Sigma), and homogenized in a Dounce homogenizer. After incubation on ice for 20 min, samples were centrifuged at 10 000*g*, (4°C, 15 min), and the following cellular fractions were obtained: fraction S (supernatant), and containing soluble, partly soluble proteins and membranes; and fraction P (pellet), containing nucleus, mitochondria and accessory structures of the flagellum.

Cell fractionation

We obtained subcellular fractions of spermatozoa from the cauda epididymidis as previously described (Visconti *et al.*, 1996), with minor modifications. Briefly, spermatozoa (10–15 × 10^6 cells) were homogenized in TE buffer (50 mM Tris, 1 mM EDTA, pH 7.5) containing protease inhibitor cocktail. After centrifugation at 10 000*g* (4°C, 10 min), the resulting supernatant (S10 fraction) was centrifuged at 100 000*g* (4°C, 60 min) using a fixed-angle rotor. We obtained the following fractions: (i) P10, the pellet of the 10 000*g* centrifugation containing organelles such as nuclei, mitochondria and accessory structures of the flagellum, (ii) P100, the pellet of the 100 000*g* centrifugation containing mostly membranes and (iii) S100 the supernatant of the 100 000*g* centrifugation containing soluble proteins.

Western blot analysis

We resuspended the pellet and supernatant fractions in sample buffer supplemented or not with 50 mM TCEP [tris(2-carboxyethyl) phosphine] and size-separated by SDS-PAGE (sodium dodecyl sulfate-polyacrylamide gel electrophoresis) as previously described (Mariani *et al.*, 2020). Proteins were transferred from the gel to a polyvinylidene difluoride membrane, and protein transfer was confirmed by Amido Black staining.

Membranes were incubated with blocking solution [5% w/v milk in TBS-T buffer (100 mM Tris-HCl pH 8.0, 150 mM NaCl, 0.05% v/v Tween 20)] for 1.5 h, washed with TBS-T buffer, then sequentially probed with anti-EPPIN Q20E antibody (1.5 µg/ml) and anti-rabbit secondary antibody conjugated to horseradish peroxidase (0.01 µg/ml). Protein detection was obtained by chemiluminescence with ECL Super Signal West Femto (Thermo Fisher). Negative control experiments were performed in the presence of anti-EPPIN antibody pre-adsorbed with a 10-fold molar excess of recombinant EPPIN. Anti-ACTB (actin beta) rabbit monoclonal antibody (Cell Signaling, Danvers, MA, USA, cat. #4970S, 1:1000) was used as an endogenous control.

Immunofluorescence

We performed immunofluorescence assays using spermatozoa isolated from cauda epididymidis submitted or not to capacitation. Experiments were performed in buffers supplemented or not with 0.02% w/v saponin to obtain permeabilized and non-permeabilized cells, respectively (Jamur and Oliver, 2010). Briefly, paraformaldehyde-fixed air-dried sperm smears were incubated with blocking buffer (1% w/v BSA in PBS buffer) for 90 min. Smears were then incubated with one of the following anti-EPPIN antibodies: S21C (1.5 µg/ml), F21C (2.0 µg/ml) or Q20E (5 µg/ml) diluted in blocking buffer overnight at

4°C. Smears were washed and incubated with Alexa Fluor 594-conjugated anti-rabbit secondary antibody (10 µg/ml) for 60 min. DAPI (4,6-diamidino-2-phenylindole) was used for nuclear staining. Images were captured and documented with appropriate excitation filters with a digital photomicroscope Axiophot II (Zeiss, Jena, Germany). The final pictures were chosen to represent the pattern of EPPIN-positive staining routinely observed in immunofluorescence experiments and subjected to the same brightness/contrast adjustments by Image J software version 1.52a (Rueden *et al.*, 2017).

Analysis of sperm motility

We diluted the sperm suspension (2×10^5 cells/ml; final volume 150 µl) with HTF medium containing anti-EPPIN S21C, F21C or Q20E antibodies or their respective Fab fragments (0.4–0.6 mg/ml) in 12 × 75 mm glass tubes at 37°C and 5%/95% CO_2/air. Sperm suspensions were incubated in the absence of anti-EPPIN antibodies (HTF only), and pre-immune serum (PIS) or normal rabbit IgG Fab fragments (0.4–0.6 mg/ml) were used as controls.

We evaluated sperm motility by computer-assisted sperm analysis using a CEROS II system (Hamilton-Thorne, Beverly, MA, USA), including Animal Motility-II Software version 1.9, and an Olympus CX41 microscope equipped with a MiniTherm stage warmer and a JAI CM-040 digital camera. We placed aliquots of diluted sperm suspension into pre-warmed 80-µm 2XCELL slides (Hamilton-Thorne) at 37°C using large-bore pipette tips, and evaluated sperm motility 30, 60 and 120 min after incubation. Time-point zero was considered 2 min after incubation of spermatozoa with anti-EPPIN antibodies. Sperm tracks (1.5 s, 90 frames) were captured with a frame rate acquisition of 60 Hz and 4× negative-phase contrast objective. We recorded at least 200 spermatozoa and 10 fields for each sample analyzed. The video playback was used to analyze sperm tracks individually and remove mistracked spermatozoa, which may occur owing to cell–cell or cell–debris collisions and false-negative debris detection. We retrieved individual ASCII files containing individual sperm track details for every analysis made. Sperm tracks with <45 (50%) acquisition points were removed from subsequent analyses (Goodson *et al.*, 2011).

We evaluated the following sperm kinematic parameters: average path velocity (VAP; µm/s), straight-line velocity (VSL; µm/s), curvilinear velocity (VCL; µm/s), amplitude of lateral head (ALH; µm), straightness (STR, %) and linearity (LIN; %). We classified tracks as progressive if VAP > 50 µm/s and STR > 50%, and as hyperactivated if VCL ≥ 180 µm/s, ALH ≥ 9.5 µm and LIN < 23.6%; Kawano *et al.*, 2014; Ernesto *et al.*, 2015). The percentage sperm motility (%motility) and VSL were used to calculate the normalized index of relative motility inhibition (RMI, %motility*VSL of sample/%motility*VSL of control) (Silva *et al.*, 2013). The ALH and VCL were used to calculate the normalized DANCE (VCL*ALH of sample/VCL*ALH of control; Alquézar-Baeta *et al.*, 2019).

In vitro fertilization

We performed IVF as previously described (Summers *et al.*, 2000), with minor modifications. Swiss male mice of proven fertility were killed and their cauda epididymidis were dissected in 1.0 ml of KSOMaa medium (95 mM NaCl, 2.5 mM KCl, 0.35 mM KH_2PO4, 0.2 mM $MgSO_4$, 0.2 mM glucose, 25 mM $NaHCO_3$, 1.7 mM $CaCl_2$, 0.2 mM sodium pyruvate, 10 mM sodium lactate, 0.01 mM EDTA, 1 mM L-glutamine, containing 0.6% w/v BSA, 1% v/v minimal essential medium essential amino acids and 0.5% v/v non-essential amino acid) to release spermatozoa into the medium. Pools of spermatozoa (2.0×10^5 cells) were diluted in 200 µl KSOMaa droplets (final concentration 1.0×10^6 cells/ml) in the absence (control) or presence of normal rabbit IgG (IgG control), Q20E or S21C antibodies (0.1 mg/ml). Sperm suspensions were covered with pre-warmed mineral oil and incubated for 60 min at 37°C (5%/95% CO_2/air) to induce sperm capacitation.

CB6F1 females were superovulated with 5 IU PMSG (pregnant mare serum gonadotropin) and 5 IU hCG by intraperitoneal injection 48 h apart. Females were killed 12–15 h post-hCG injection, and their oviductal ampullae containing ovulated cumulus-oocyte complexes (COCs) were collected in KSOMaa. Pools of 20–40 COCs were transferred to IVF droplets containing spermatozoa capacitated in fresh KSOMaa or containing rabbit IgG, Q20E or S21C antibodies. The IVF dish was incubated for 6 h in 5% CO_2 in a humid chamber at 37°C. After IVF, COCs were denuded by gentle pipetting, and presumptive zygotes were washed and cultured in KSOMaa in 5% CO_2 and high humidity at 37°C. Fertilization rates were determined at 24 h after IVF (cleavage rates), and total embryonic development was determined at 96 h after IVF (morulae and blastocysts).

Analysis of sperm capacitation-induced tyrosine phosphorylation

We diluted aliquots of sperm suspension (5.0×10^6 cells/ml) in capacitating TYH medium in the presence of normal rabbit IgG (control, 0.3 mg/ml), or anti-EPPIN S21C or Q20E antibodies (0.01, 0.1 and 0.3 mg/ml) for 120 min at 37C (5%/95% CO_2/air). Sperm samples that had been either processed immediately after isolation from the cauda epididymidis or incubated under capacitating conditions for 120 min in TYH medium only were used as non-capacitated (NC) and capacitated (CAP) controls, respectively. Sperm samples were washed with PBS buffer pH 7.4, centrifuged at 800*g* (10 min), resuspended in sample buffer and boiled at 85°C for 5 min. After centrifugation, we collected the supernatant and separated total proteins by SDS-PAGE. We performed western blotting with mouse monoclonal anti-phosphotyrosine antibody, clone 4G10 (MerckMillipore, Burlington, MA, USA, cat. #05-321, 1 µg/ml), diluted in blocking solution containing 3% fat-free milk (w/v) in TBS-T buffer, as previously described (Alvau *et al.*, 2016). Western blot images were subjected to brightness/contrast adjustments and analyzed for pixel quantification of target phosphoprotein bands (~75 kDa) by using ImageJ software (Rueden *et al.*, 2017). The immunoreactive band corresponding to phosphohexokinase (~116 kDa) was used as endogenous control. Densitometric data were expressed as arbitrary units.

Statistical analysis

Results were expressed as mean ± SEM. We checked the normal distribution and homoscedasticity of the data with the Kolmogorov–Smirnov test and the *F*-test, respectively. Data that failed normality and homoscedasticity tests were transformed to Log values before parametric statistics. Percentage data were transformed to arcsine square-root transformation before statistical analysis (Zar, 2010). Student's *t*-test was performed to determine statistical differences

between two groups. ANOVA followed by Tukey test was used to determine statistical differences when more than two groups were compared. $P < 0.05$ was considered statistically significant. We performed statistical analyses with GraphPad Prism® 6.0 software (GraphPad Software Inc., San Diego, CA, USA).

Results

EPPIN is associated with sperm surface and cytoskeleton structures during post-testicular maturation

Using rodent models (i.e. rats and mice), we previously demonstrated that EPPIN distribution dynamically changes in sperm head and flagellum during epididymal transit (Silva *et al.*, 2012a,b; Mariani *et al.*, 2020). Here, we took a step further by investigating EPPIN compartmentalization in spermatozoa during two different stages of post-testicular maturation, namely epididymal maturation and capacitation.

Our western blot results showed a differential EPPIN expression pattern in Triton X-100-soluble (S) and -insoluble (P) fractions from spermatozoa isolated from different epididymal regions (Fig. 1A). Using anti-EPPIN Q20E antibody, we observed two EPPIN-positive immunoreactive bands with apparent molecular masses of ∼14 and ∼28 kDa in the S fraction of spermatozoa isolated from the caput, corpus and cauda epididymidis (Fig. 1A). We observed a different band of ∼19 kDa and higher bands in the range of ∼47–65 kDa in the P fraction of spermatozoa isolated from the corpus and cauda epididymidis, but not from the caput region (Fig. 1A). Similar results were obtained when samples were processed for SDS-PAGE in non-reducing conditions (Supplementary Fig. S1). Moreover, capacitation *in vitro* of spermatozoa isolated from the cauda epididymidis did not affect the pattern of EPPIN-positive immunoreactive bands in comparison with non-capacitated spermatozoa (Supplementary Fig. S1). We detected no immunoreactive bands when experiments were performed using anti-EPPIN Q20E antibody pre-adsorbed with recombinant EPPIN (Fig. 1A and Supplementary Fig. S1).

To define the presence of EPPIN in sperm cellular compartments better, we obtained subcellular fractions of mature spermatozoa by cell fractionation. Western blot analysis using TE buffer-soluble fraction (S10) revealed two major EPPIN-positive immunoreactive bands with apparent molecular masses of ∼14 and ∼28 kDa, and an additional faint band of ∼47 kDa (Fig. 1B). We further observed four bands with apparent molecular masses of ∼14, ∼19, ∼47 and ∼65 kDa in the TE buffer-insoluble fraction (P10; Fig. 1B). After ultracentrifugation of the S10 fraction, we observed that both ∼14 and ∼28 kDa bands remained in the S100 fraction, while the ∼47 kDa band was found in S100 and P100 fractions (Fig. 1B).

We next evaluated the relative stability of EPPIN distribution in spermatozoa during capacitation. Immunofluorescence assays showed a similar pattern of EPPIN-positive immunostaining in both saponin-permeabilized and non-permeabilized spermatozoa, thus confirming the presence of EPPIN on the sperm surface (Fig. 1C). Most non-capacitated spermatozoa displayed EPPIN-positive immunostaining in the anterior acrosome and equatorial segment of the head (Fig. 1C). We further observed EPPIN-positive staining in the midpiece (greater intensity) and principal piece (lower intensity) of the flagellum of non-capacitated spermatozoa (Fig. 1C). This pattern of EPPIN-positive immunostaining was similar in capacitated spermatozoa regardless of cell permeabilization with saponin (Fig. 1C). Moreover, we obtained similar results when saponin-permeabilized and non-permeabilized spermatozoa were stained with anti-EPPIN S21C and F21C antibodies (Supplementary Fig. S2). These results demonstrated that Q20E, S21C and F21C epitopes are available for antibody binding on the mouse sperm surface and that EPPIN remains associated with capacitated spermatozoa.

Antibodies mapping epitopes in EPPIN WFDC and Kunitz domains differentially inhibited mouse sperm motility

We investigated the effects of three anti-EPPIN antibodies mapping distinct epitopes in EPPIN C-terminal (F21C and S21C antibodies) and N-terminal (Q20E antibody) regions on mouse sperm motility. F21C antibody (0.4 mg/ml) did not affect any motility parameter, except by an increase in progressive motility at 60 min (>31%, $P = 0.041$) of incubation (Supplementary Fig. S3).

On the other hand, S21C antibody (0.4 mg/ml) inhibited motility at 60 min (<25%, $P = 0.005$) and 120 min (<25%, $P = 0.011$) of incubation in comparison with PIS control (Fig. 2A). S21C antibody further inhibited progressive motility, which was manifested earlier at 30 min (<40%, $P = 0.009$) and persisted until 60 min (<40%, $P = 0.003$) of incubation (Fig. 2A). These results were consistent with a readily detectable reduction on the length of sperm tracks in S21C antibody-treated samples in comparison with PIS control (Supplementary Fig. S4 and Videos S1 and S2). Moreover, S21C antibody inhibited hyperactivated motility at 120 min (<85%, $P = 0.002$; Fig. 2A). To address whether S21C-induced inhibition of sperm motility was dependent on bivalent or monovalent interaction with its epitope, we incubated mouse spermatozoa with S21C antibody Fab fragments [S21C(Fab)]. We observed that S21C(Fab) (0.5 mg/ml) inhibited sperm motility (30 min: <29%, $P = 0.0002$; 60 min: <43%, $P = 0.001$; and 120 min: <57%, $P = 0.0001$) and progressive motility (30 min: <55%, $P = 0.004$; 60 min: <58%, $P = 0.032$; and 120 min: <74%, $P = 0.001$) at all time-points analyzed in comparison with control samples incubated with normal rabbit IgG Fab fragments [IgG(Fab)] (Fig. 2B and Supplementary Fig. S4). Consistently, S21C(Fab) inhibited hyperactivated motility at 120 min (<71%, $P = 0.018$) of incubation (Fig. 2B).

Anti-EPPIN Q20E antibody-induced milder effects on sperm motility compared with S21C antibody. Q20E antibody (0.6 mg/ml) did not change sperm motility from the PIS control, except by an inhibition of progressive motility at 30 min (<37%, $P = 0.008$) and 60 min (<49%, $P = 0.014$) after incubation (Fig. 2C and Supplementary Video S3). On the other hand, Q20E Fab fragments [Q20E(Fab), 0.6 mg/ml] inhibited both motility (60 min: <26%, $P = 0.023$; and 120 min: <35%, $P = 0.005$) and progressive motility (60 min: <38%, $P = 0.021$; and 120 min: <41%, $P = 0.010$) at 60 and 120 min after incubation (Fig. 2D and Supplementary Fig. S4). Neither Q20E antibody nor Q20E(Fab) affected hyperactivated motility (Fig. 2C and D).

Antibodies mapping epitopes in EPPIN WFDC and Kunitz domains differentially modulated mouse sperm kinematics

We further evaluated the effects of anti-EPPIN antibodies on sperm kinematics parameters driving progressive (VAP, VSL and STR) and

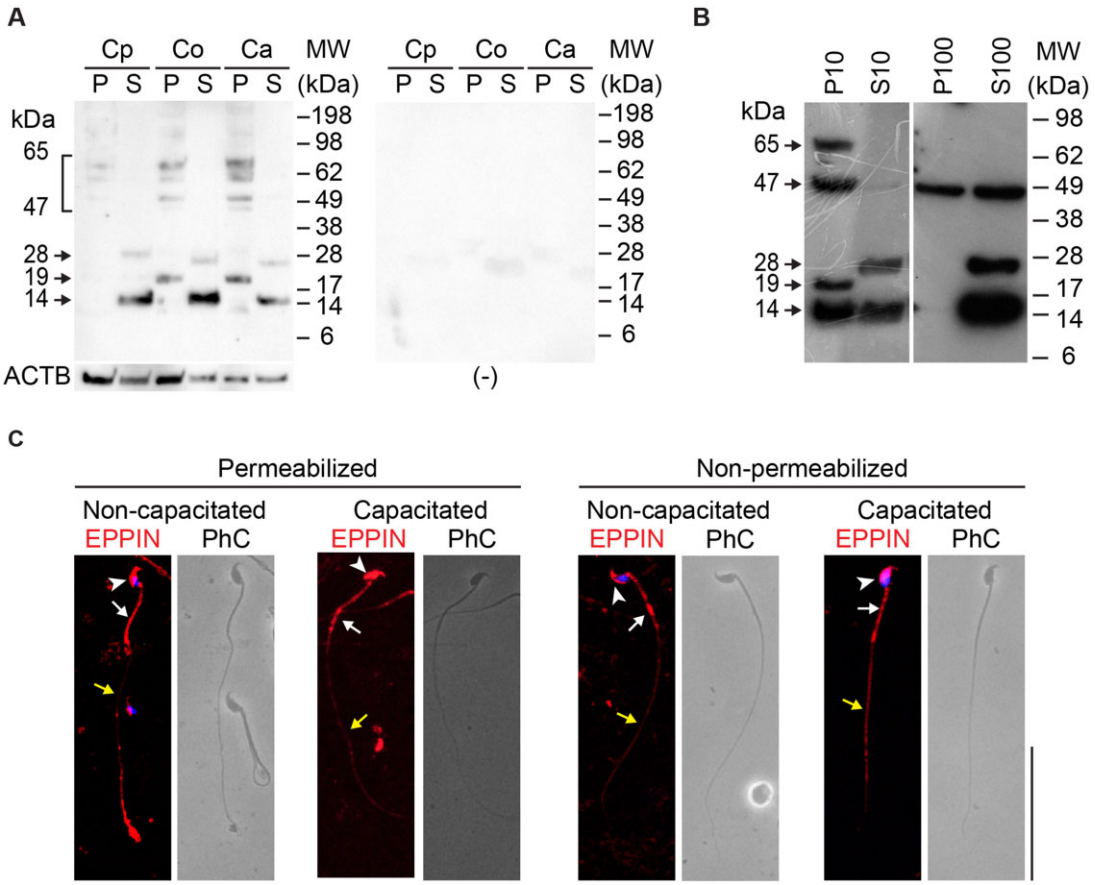

Figure 1. Impact of post-testicular maturation on epididymal protease inhibitor (EPPIN) expression in mouse spermatozoa. (**A**) EPPIN expression in Triton X-100 insoluble (P) and soluble (S) fractions of spermatozoa isolated from the caput (Cp, including the initial segment), corpus (Co) and cauda (Ca) epididymidis by western blot. Actin beta (ACTB) was used as an endogenous control. Negative control (−) was performed with primary antibody pre-adsorbed with recombinant EPPIN. (**B**) EPPIN expression in subcellular fractions of spermatozoa isolated from the cauda epididymidis. P10 and S10 indicate TE buffer soluble and insoluble fractions, respectively, after centrifugation. P100 and S100 indicate S10 soluble and insoluble fractions after ultracentrifugation. Membranes were probed with Q20E antibody. Arrows indicate EPPIN-positive immunoreactive bands. MW indicates a standard protein ladder (kDa). (**C**) EPPIN-positive immunostaining (red) in non-capacitated and capacitated mouse spermatozoa. Immunofluorescence experiments were performed in the presence or absence of saponin to obtain permeabilized (left panel) and non-permeabilized (right panel) spermatozoa. EPPIN-positive-immunostaining was detected on the head (arrowhead), midpiece (white arrow) and principal piece (yellow arrow) of the flagellum. Cell nuclei were stained with DAPI (blue). PhC, Phase contrast. Scale bar: 50 µm. Results are representative of independent experiments performed with sperm samples from five (**A**) and three (**B**, **C**) mice.

vigorous (VCL, ALH and LIN) movements (Cancel *et al.*, 2000). F21C antibody did not change sperm kinematic parameters, except by an increase in VSL (>31%, $P = 0.046$) and STR (>37%, $P = 0.045$) at 120 min (Supplementary Fig. S3). Conversely, S21C antibody inhibited VSL at 30 min (<40%, $P = 0.016$) and both VSL and VAP at 60 min (VSL: <35%, $P = 0.020$, VAP: <28%, $P = 0.036$) of incubation (Fig. 3A). S21C-induced inhibition of VAP, but not VSL, persisted at 120 min (<26%, $P = 0.047$). At this later time-point, S21C antibody further increased STR (>78%, $P = 0.002$; Fig. 3A). Incubation of spermatozoa with S21C(Fab) induced similar outcomes on VAP (60 min: <30%, $P = 0.033$; 120 min: <37%, $P = 0.003$), VSL (30 min: <35%, $P = 0.046$; 60 min: <40%, $P = 0.048$, 120 min: <33%, $P = 0.048$), but did not affect STR (Fig. 3B).

Kinematic parameters associated with vigorous sperm motility were also affected by S21C antibody, as demonstrated by a decrease in VCL and ALH at 60 min (VCL: <30%, $P = 0.039$, ALH: <32%, $P = 0.045$) and 120 min (VCL: <26%, $P = 0.043$, ALH: <31%, $P = 0.045$), in parallel to an increase in LIN at 120 min (>64%, $P = 0.001$) of incubation (Fig. 3A). S21C(Fab) induced a similar decrease in ALH at all time-points (30 min: <18%, $P = 0.039$; 60 min: <24%, $P = 0.033$, 120 min: <37%, $P = 0.0002$) and in VCL at 120 min (<38%, $P = 0.003$) of incubation (Fig. 3B). However, S21C(Fab) decreased LIN at 30 min (<21%, $P = 0.048$) of incubation but not at later time-points (Fig. 3B).

Consistent with the effects induced in sperm progressive motility, Q20E antibody decreased VAP (<19%, $P = 0.022$) and increased SRT

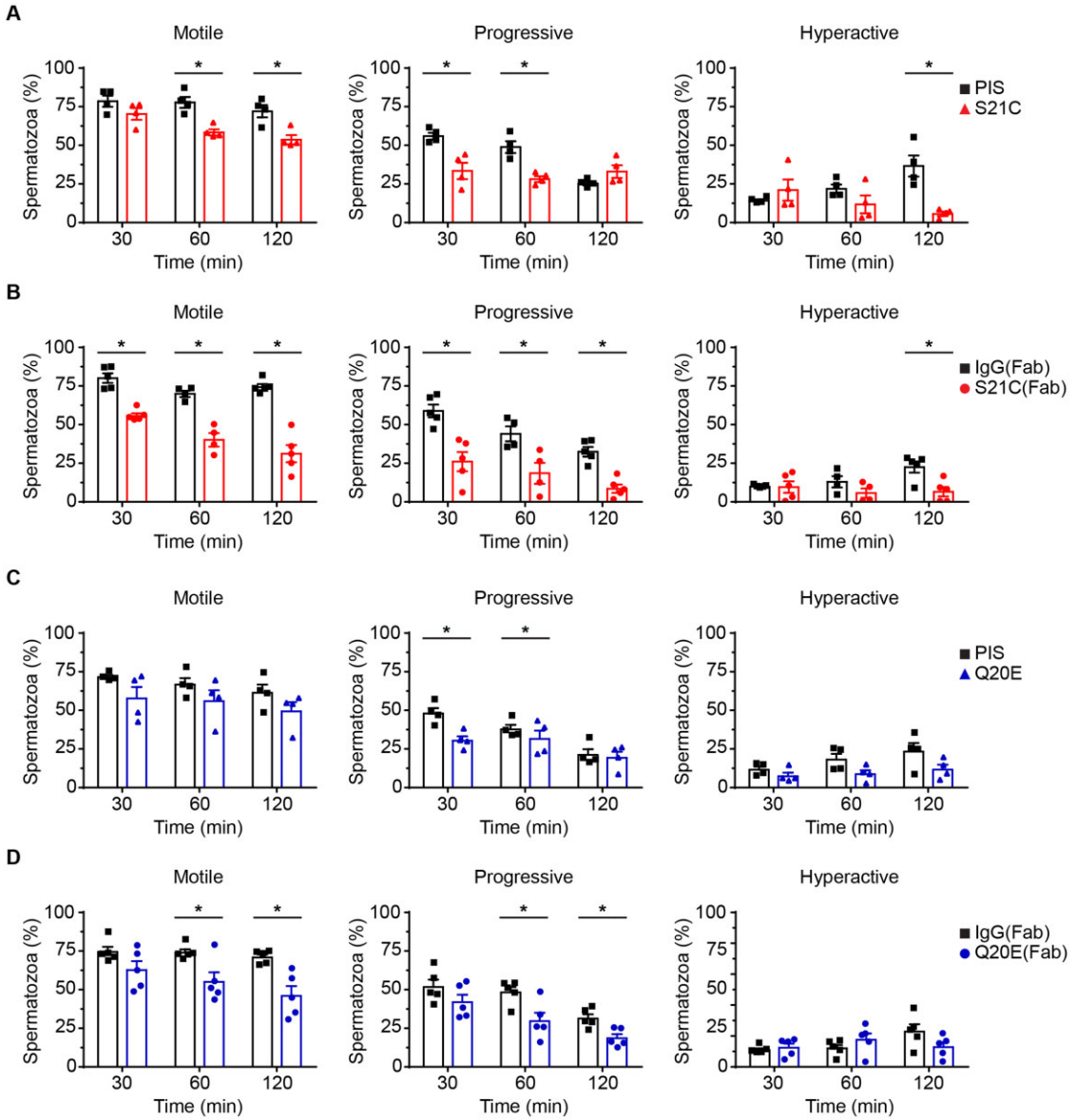

Figure 2. Effects of anti-epididymal protease inhibitor S21C and Q20E antibodies on mouse sperm motility. (**A**, **B**) Motility of spermatozoa incubated with S21C antibody (0.4 mg/ml), or its Fab fragment [S21C(Fab), 0.5 mg/ml]. (**C, D**) Motility of spermatozoa incubated with Q20E antibody (0.6 mg/ml), or its Fab fragment [Q20E(Fab), 0.6 mg/ml]. Spermatozoa incubated with pre-immune serum (PIS) or normal rabbit IgG Fab fragments [IgG(Fab)] under the same conditions were used as controls. Sperm motility was evaluated 30, 60 and 120 min after incubation. *Indicates statistically different from control groups ($P < 0.05$; Student's *t*-test). Percentage data were converted to arcsine square-root values before statistical analysis. Results represent mean ± SEM from independent experiments performed with sperm samples from four to five mice (shown by points).

(>17%, $P = 0.044$) at 30 and 120 min of incubation, respectively (Fig. 4A). We further observed that Q20E antibody decreased VCL at 30 min (<20%, $P = 0.022$) and ALH at 30 min (<23%, $P = 0.006$), which showed a trend toward control values at 60 min (<19%, $P = 0.048$) of incubation (Fig. 4A). Moreover, Q20E antibody induced a later increase in LIN at 120 min (>20%, $P = 0.044$; Fig. 4A). Q20E(Fab), however, did not reproduce the effects of Q20E antibody on sperm kinematics parameters; we did not observe any effect of Q20E(Fab), except a decrease in ALH (<17%, $P = 0.026$) at 120 min of incubation (Fig. 4B).

The negative impact of S21C antibody on sperm motility and kinematic parameters caused a ~2-fold decrease in the normalized index of RMI at 30 min ($P = 0.037$) and 60 min ($P = 0.001$; Fig. 5A). Moreover, S21C antibody induced a ~2-fold decrease in the normalized DANCE parameter at 60 min ($P = 0.001$) and 120 min ($P = 0.003$) of incubation (Fig. 5A). We obtained similar results when spermatozoa were incubated with S21C(Fab), which decreased normalized RMI at all time-points (30 min: <2-fold, $P = 0.012$, 60 min: <3-fold, $P = 0.009$, and 120 min: <5-fold, $P < 0.0001$) and normalized

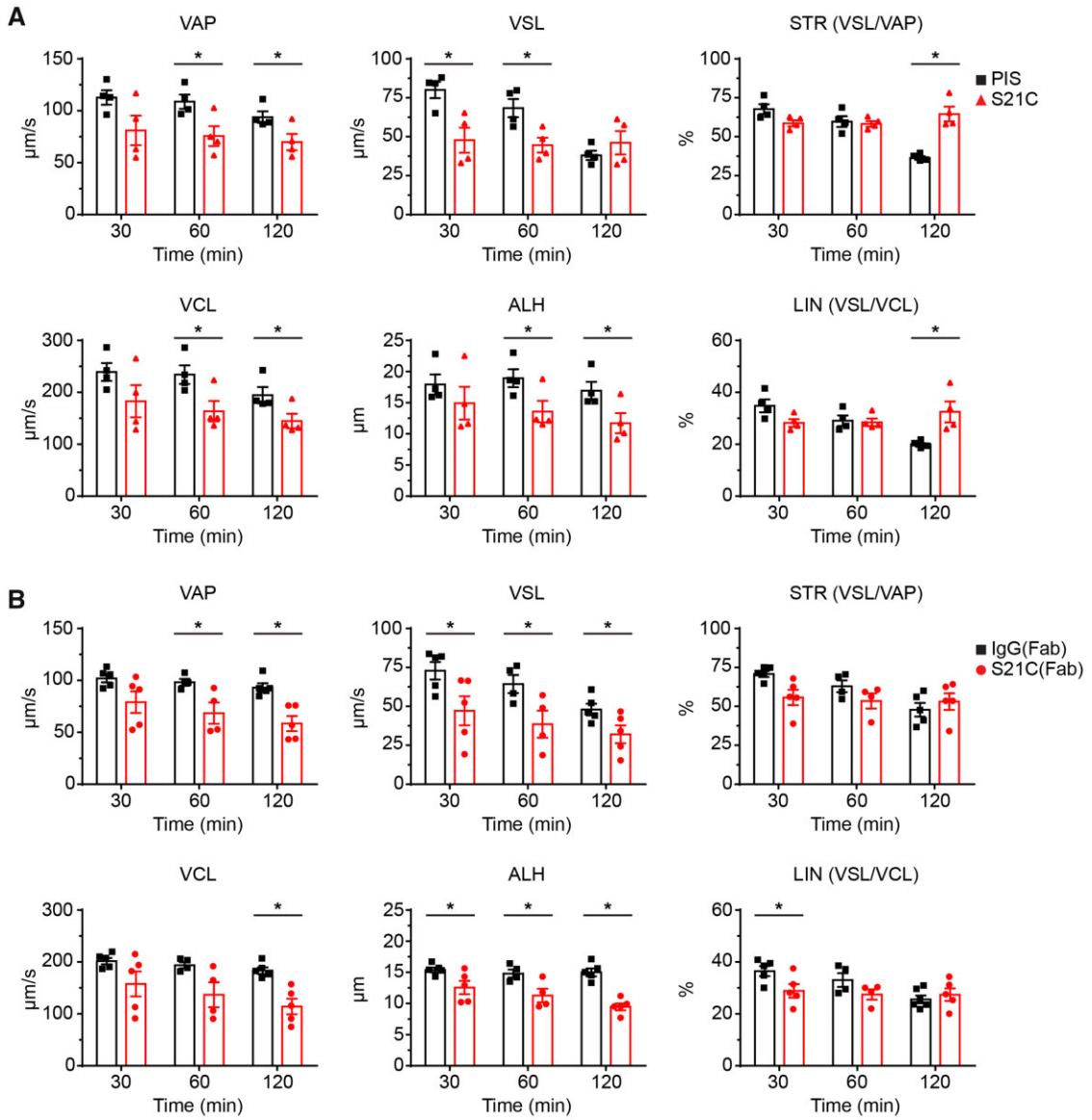

Figure 3. Effects of anti-epididymal protease inhibitor S21C antibody on mouse sperm kinematics parameters. (**A**) Kinematic parameters of spermatozoa incubated with S21C antibody (0.4 mg/ml). (**B**) Kinematic parameters of spermatozoa incubated with S21C Fab fragment [S21C(Fab)] (0.5 mg/ml). Spermatozoa incubated with pre-immune serum (PIS) or normal rabbit IgG Fab fragments [IgG(Fab)] under the same conditions were used as controls. Sperm kinematics was evaluated 30, 60 and 120 min after incubation. VAP, average path velocity; VSL, straight-line velocity; STR, straightness; VCL, curvilinear velocity; ALH, amplitude of lateral head displacement; LIN, linearity. *Indicates statistically different from control groups ($P < 0.05$; Student's *t*-test). Percentage data were converted to arcsine square-root values before statistical analysis. Results represent mean ± SEM from independent experiments performed with sperm samples from four to five mice (shown by points).

DANCE at 60 min (<2-fold, $P = 0.037$) and 120 min (<3-fold, $P = 0.003$; Fig. 5B). Regarding Q20E antibody, we observed no effects on normalized RMI, while normalized DANCE was decreased at 30 min (<1.6-fold, $P = 0.011$) of incubation, an effect that did not persist at later time-points (Fig. 5C). On the other hand, Q20E(Fab) decreased in normalized RMI (<1.7-fold, $P = 0.004$) and normalized DANCE (<1.4-fold, $P < 0.0009$) at 120 min of incubation (Fig. 5D).

Antibodies mapping epitopes in EPPIN WFDC and Kunitz domains impaired sperm fertilizing ability but not capacitation-induced tyrosine phosphorylation

To evaluate whether inhibition of sperm motility parameters induced by S21C and Q20E antibodies affects sperm fertilizing ability, we

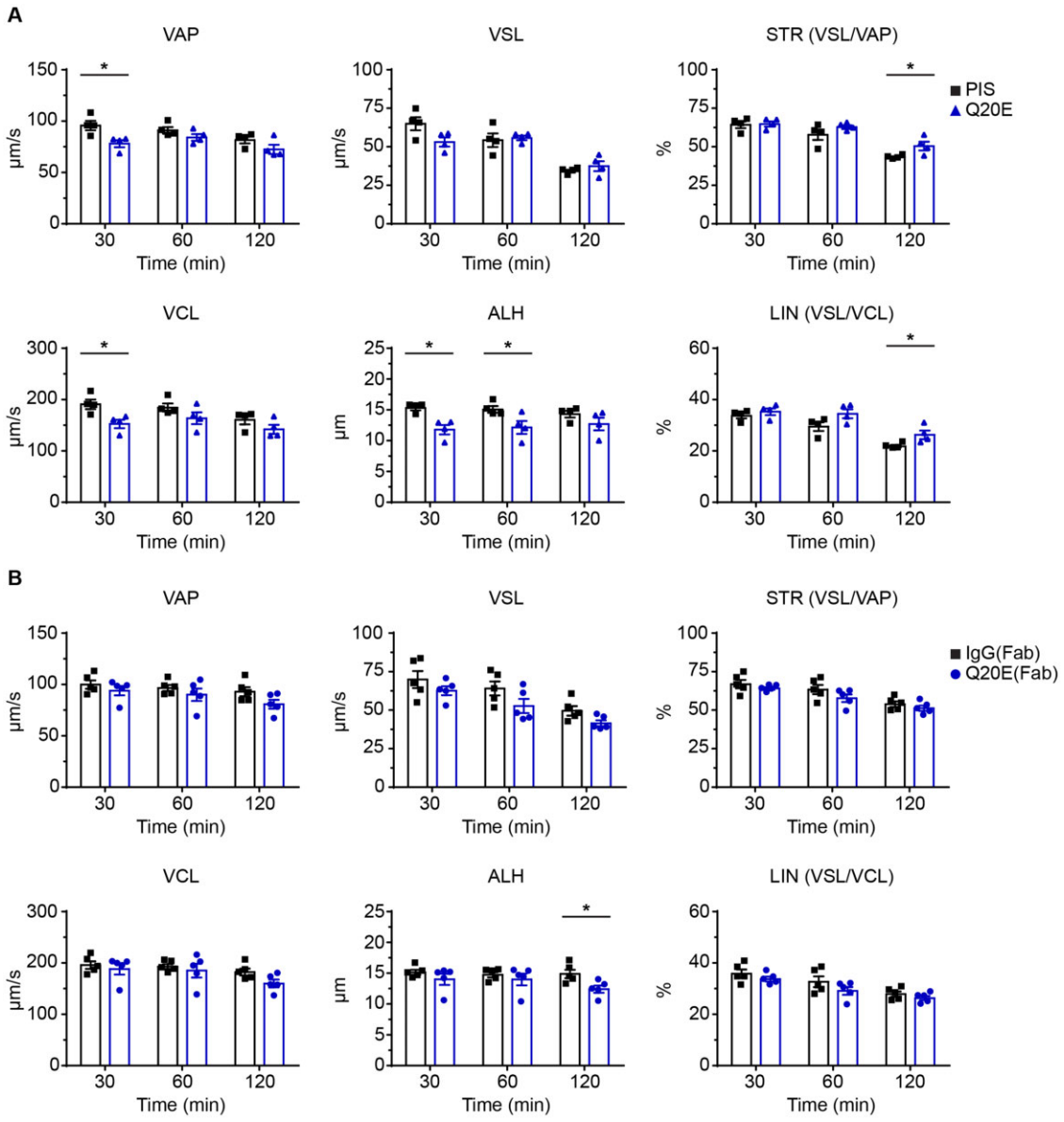

Figure 4. Effects of anti-epididymal protease inhibitor Q20E antibody on mouse sperm kinematics parameters. (**A**) Kinematic parameters of spermatozoa incubated with Q20E antibody (0.6 mg/ml). (**B**) Kinematic parameters of spermatozoa incubated with Q20E Fab fragment [Q20E(Fab)] (0.6 mg/ml). Spermatozoa incubated with pre-immune serum (PIS) or normal rabbit IgG Fab fragments [IgG(Fab)] under the same conditions were used as controls. Sperm kinematics was evaluated 30, 60 and 120 min after incubation. *Indicates statistically different from control groups ($P < 0.05$; Student's *t*-test). Percentage data were converted arcsine square-root values before statistical analysis. Results represent mean ± SEM from independent experiments performed with sperm samples from four to five mice (shown by points).

performed IVF. Our results demonstrated that incubation of spermatozoa during capacitation in the presence of normal rabbit IgG (0.1 mg/ml) did not affect their fertilizing ability compared with fresh medium control (CTL), as revealed by similar cleavage rates on post-IVF Day 1 (average ± SEM—CTL: 84% ± 3% vs. IgG: 88% ± 2%; $P = 0.890$) and total embryonic development on post-IVF Day 4 (CTL: 67% ± 2% vs. IgG: 64% ± 2%, $P = 0.996$). Under the same conditions, we observed a decrease in cleavage rates when spermatozoa were incubated with S21C (<30%, $P = 0.008$) and Q20E antibodies (<25%, $P = 0.021$) in comparison with IgG control (Fig. 6A).

To gain further insights into the mechanisms by which S21C and Q20E antibodies disturb sperm function, we investigated whether they affected capacitation-induced sperm protein tyrosine phosphorylation. We first confirmed the time-dependent increase in tyrosine phosphorylation of sperm proteins induced by capacitation *in vitro* (Visconti *et al.*, 1995a; Supplementary Fig. S5).

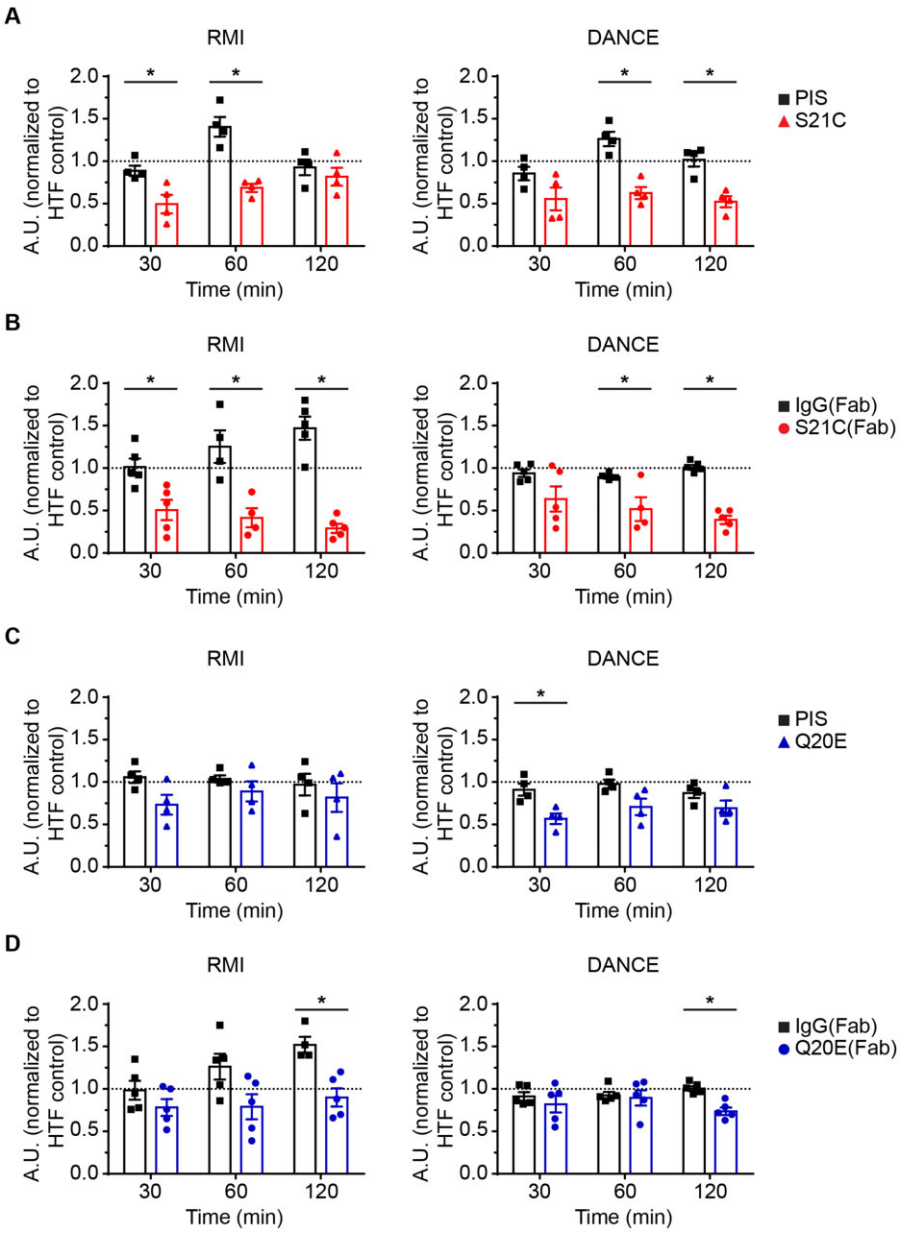

Figure 5. Effects of anti-epididymal protease inhibitor S21C and Q20E antibodies on motility indexes measuring progressive (relative motility inhibition, RMI; %motility × average path velocity, VSL) and vigorous (DANCE; curvilinear velocity, VCL × amplitude of lateral head, ALH) movements in mouse spermatozoa. (**A, B**) Normalized RMI and normalized DANCE of spermatozoa incubated with S21C antibody (0.4 mg/ml), or its Fab fragment [S21C(Fab), 0.5 mg/ml]. (**C, D**) Normalized RMI and normalized DANCE of spermatozoa incubated with Q20E antibody (0.6 mg/ml), or its Fab fragment [Q20E(Fab), 0.6 mg/ml]. Spermatozoa incubated with pre-immune serum (PIS) or normal rabbit IgG Fab fragments [IgG(Fab)] under the same conditions were used as controls. Normalized RMI and normalized DANCE were calculated using sperm motility data acquired 30, 60 and 120 min after incubation. Normalized RMI was calculated as (%motility*VSL of sample/%motility*VSL of control). Normalized DANCE was calculated as (VCL*ALH of sample/VCL*ALH of control). A.U. indicates arbitrary units. *Indicates statistically different from PIS group ($P < 0.05$; Student's *t*-test). Results represent mean ± SEM from independent experiments performed with sperm samples from four to five mice (shown by points).

The intensity of phosphotyrosine-positive bands increased over time, reaching the highest levels between 60 and 120 min (Supplementary Fig. S5). Spermatozoa incubated for 120 min under capacitating conditions in the presence of S21C or Q20E (0.01, 0.1 and 0.3 mg/ml) did not show changes in phosphotyrosine profile in comparison with IgG control (0.3 mg/ml; Fig. 6B and C).

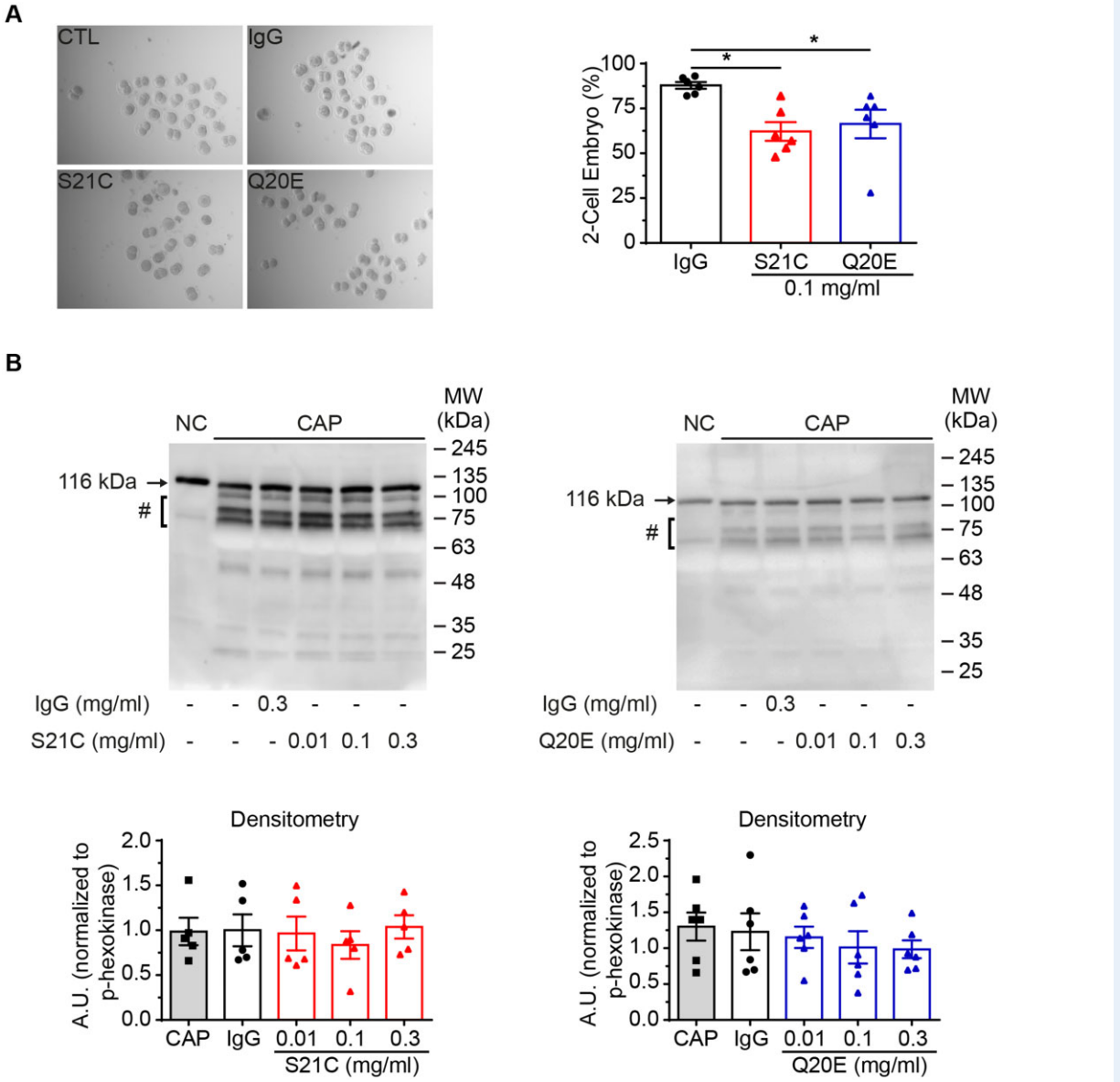

Figure 6. Effects of anti-epididymal protease inhibitor S21C and Q20E antibodies on sperm capacitation-associated events. (**A**) Cleavage rates of mouse oocytes after *in vitro* insemination with spermatozoa incubated under capacitating conditions in the presence of S21C or Q20E antibodies (0.1 mg/ml). Spermatozoa incubated under capacitating conditions in medium only or the presence of normal rabbit IgG (0.1 mg/ml) were used as controls. Results were expressed as percentage of two-cell embryos to the total number of cumulus-oocyte complexes per fertilization drop. Results represent mean ± SEM from independent experiments performed with sperm samples from six mice (shown by points). (**B**) Phosphotyrosine profile of mouse spermatozoa incubated under capacitating conditions in the presence of increasing concentrations of S21C or Q20E antibodies (0.01, 0.1 and 0.3 mg/ml) 120 min. Spermatozoa immediately processed after isolation in non-capacitating conditions (NC) or incubated under capacitating conditions for 120 min (CAP) in capacitating medium only or in the presence of normal rabbit IgG (0.3 mg/ml) were used as controls. Sperm total protein extracts (1.0×10^6 cells/lane) were analyzed for tyrosine phosphorylation with anti-phosphotyrosine antibody. Results were analyzed using ImageJ, and pixels for each lane at the double band ~75 kDa (#) were quantified using phosphohexokinase (arrow) bands as endogenous control. MW indicates a standard protein ladder (kDa). Results represent mean ± SEM from independent experiments performed with sperm samples from five to six mice (shown by points).

Discussion

Pharmacological approaches targeting EPPIN have the potential to generate a novel class of on-demand, fast-onset, non-hormonal male contraceptive drugs with spermostatic activity (O'Rand *et al.*, 2016; Drevet, 2018). Previous studies have established that the EPPIN C-terminal region, containing the Kunitz domain, provides a binding surface for SEMG1 on human spermatozoa, resulting in transient inhibition of motility and capacitation after ejaculation (Wang *et al.*, 2005; Silva *et al.*, 2012a,b; O'Rand *et al.*, 2016). For this reason, studies on EPPIN ligands as sperm motility inhibitors are based on compounds that bind to the EPPIN Kunitz domain (O'Rand *et al.*, 2011, 2016, 2018). Nevertheless, recent studies on full-length EPPIN homology models indicated that amino acid residues in both WFDC and Kunitz domains may play roles in EPPIN interaction with SEMG1 and its small molecular weight ligand EP055 (Shan *et al.*, 2019). These findings suggest that the EPPIN N- and C-terminal regions could contribute to the regulation of sperm function. Using anti-EPPIN antibodies as pharmacological tools, we showed that the EPPIN Kunitz domain plays a major role in governing progressive and vigorous movements of mouse spermatozoa, but its WFDC domain may also contribute to these outcomes. The negative effects of anti-EPPIN S21C and Q20E antibodies on motility parameters were associated with impairment in sperm fertilizing ability, further demonstrating that antibody-mediated EPPIN blockade on mouse spermatozoa could decrease male fertility. Our study sheds new light on the understanding of relative contributions of EPPIN WFDC and Kunitz domains on the regulation of sperm function, which may contribute to the rational design of EPPIN-binding drugs with potential clinical applications as male contraceptives.

Our previous studies in rats and mice showed that EPPIN localization in spermatozoa dynamically changes during epididymal maturation, becoming more abundant in the head and flagellum of spermatozoa isolated from distal regions of the epididymis (corpus and cauda; Silva *et al.*, 2012a,b; Mariani *et al.*, 2020). Our results herein support these observations, as we detected EPPIN-positive bands in Triton X-100-insoluble and -soluble fractions from spermatozoa isolated from the corpus and cauda epididymidis, but not from the caput region. Moreover, EPPIN-positive immunoreactive bands were differentially associated with cellular fractions of mouse spermatozoa, suggesting that EPPIN may be involved in different events governing sperm function. The ~19 kDa band was restricted to the Triton X-100-insoluble fraction from mature spermatozoa, indicating its association with sperm cytoskeleton and accessory flagellar structures (Visconti *et al.*, 1996). In parallel, we detected EPPIN as a monomer (~14 kDa band) and dimer (~28 kDa band) in the Triton X-100 soluble fraction regardless of sperm maturation stage.

Interestingly, the ~14 and ~28 kDa bands were also present in TE buffer-soluble fraction (S10), suggesting they are soluble proteins associated with the plasma membrane. To investigate this possibility, we performed cell fractionation of the S10 fraction from mature spermatozoa by ultracentrifugation. The presence of ~14 and ~28 kDa bands in the S100 fraction indicated that EPPIN monomers and dimers are either soluble or loosely bound to sperm membranes. We detected a ~47 kDa EPPIN-positive immunoreactive band, which likely represents EPPIN oligomers, in the sperm membrane-enriched fraction (P100), even in the presence of reducing agents. Interactions between EPPIN and the sperm plasma membrane likely facilitate EPPIN oligomerization via intramolecular and intermolecular bonds between residues in WFDC and Kunitz domains (Richardson *et al.*, 2001; Shan *et al.*, 2019). We consistently detected EPPIN-immunopositive staining in non-permeabilized spermatozoa. These findings show that epididymal maturation but not capacitation influence EPPIN association with different cellular compartments of spermatozoa. How EPPIN is directed to the membrane or flagellar structures; however, remains unknown. The nature of the compartmentalized expression of EPPIN in spermatozoa and its impact on sperm function warrants further investigation.

The acquisition of sperm motility is an essential event for mammalian reproduction (Turner, 2006; Freitas *et al.*, 2017). Poor sperm motility is a relevant cause of human male infertility and can only be defeated by assisted reproductive techniques (Turner, 2006). On the other hand, targeting the mechanisms governing sperm motility offers excellent opportunities to develop male contraceptives based on loss of sperm function. EPPIN's pivotal role in regulating sperm motility and druggable properties became milestones for its development as a male contraceptive drug target (O'Rand *et al.*, 2016, 2018). In an immunocontraception study, O'Rand *et al.* (2004) demonstrated that active immunization with human recombinant EPPIN in monkeys resulted in reversible infertility due to anti-EPPIN antibodies-induced inhibition of sperm motility. Further analyses on monkey anti-EPPIN contraceptive antibodies led to the identification of two dominant epitope sequences: Gln20-Arg32 and Thr102-Gln118, which are part of EPPIN WFDC and Kunitz domains, respectively (O'Rand *et al.*, 2004). Anti-EPPIN antibodies targeting the C-terminal epitope inhibited SEMG1 binding and human sperm motility (O'Rand *et al.*, 2009; Silva *et al.*, 2012a,b). Whether the EPPIN N-terminal region is involved in these events is not known.

To gain new insights into the contributions of EPPIN WFDC and Kunitz domains on the regulation of sperm motility, we investigated the effects of three affinity-purified anti-EPPIN antibodies targeting sequences in N-terminal (Q20E) and C-terminal (S21C and F21C) contraceptive epitopes in mouse spermatozoa. It is worth noting that EPPIN epitopes recognized by Q20E, S21C and F21C antibodies are exposed on the sperm surface since our immunofluorescence experiments showed intense EPPIN-positive immunostaining in the head and flagellum of non-permeabilized spermatozoa. Our results showed that S21C antibody, but not F21C antibody, negatively affected mouse sperm motility and kinematics parameters, confirming the critical roles of the Kunitz domain for the regulation of sperm motility. Given the differential effects of S21C and F21C antibodies on sperm motility and the partial overlap of their epitopes, we hypothesize that the sequence Gln111–Asn122 contains the residues critical for EPPIN control of sperm motility. This hypothesis is supported by: (i) active immunization of male mice targeting EPPIN Asn113–Asn122 peptide sequence resulted in inhibition of sperm motility and subfertility (Chen *et al.*, 2009; Sun *et al.*, 2010), (ii) EPPIN residues Asn114 and Asn116 form hydrogen bonds with SEMG1 and the EPPIN ligands B4 and EP055, which possess sperm motility inhibitory activity (O'Rand *et al.*, 2016; Shan *et al.*, 2019) and (iii) the EPPIN sequence Gln111–Asn122 is highly conserved among primates and rodents (Supplementary Fig. S6).

The proper regulation of progressive motility acquisition and its transition to hyperactivated motility is crucial for sperm fertilization potential (Suarez, 2008). Our results show that the S21C antibody inhibits both progressive and hyperactivated motilities, indicating that it disturbs signaling pathways governing these motility patterns. These

effects were consistent with S21C-induced changes in kinematic parameters associated with progressive (VAP, VSL and STR) and vigorous (VCL, ALH and LIN) sperm movements. Interestingly, S21C Fab fragments reproduced these outcomes, showing that monovalent binding to its epitope is sufficient to affect progressive motility and hyperactivated motility. Consistent with our findings, human spermatozoa incubated with S21C antibody (whole IgG and Fab fragment) display reduced progressive motility, VCL and ALH (O'Rand and Widgren, 2012). The effects of the S21C antibody on progressive and vigorous human sperm motility parameters were associated with acidification of intracellular pH and subsequent decrease in intracellular calcium levels (O'Rand and Widgren, 2012); both events are known to impair progressive motility and hyperactivation (Ho and Suarez, 2001; Carlson *et al.*, 2003). Blocking the S21C epitope likely induces a similar disruption of signaling pathways regulating intracellular calcium levels in mouse spermatozoa. Our results further underscore the functional conservation of EPPIN as a key sperm-binding molecule regulating sperm motility patterns in humans and mice, making the latter a useful model system for the preclinical evaluation of novel EPPIN ligands as male contraceptives.

Molecular docking studies have suggested that SEMG1 and EP055 interact with EPPIN residues in the Q20E antibody epitope (Shan *et al.*, 2019). Moreover, full-length EPPIN homology modeling shows that residues in the Q20E epitope (e.g., Pro30, Arg31 and Arg32) form intramolecular interactions with residues in the S21C epitope (e.g., Asn113, Ans114 and Asn116; Shan *et al.*, 2019). In agreement with these observations, we observed a mild effect of the Q20E antibody and its Fab fragment on progressive motility, indicating that the sequence Gln20-Glu39 in the EPPIN WFDC domain may also be involved in the inhibitory effects of endogenous and exogenous EPPIN ligands on sperm motility. We hypothesized that blocking the Q20E epitope disrupts the stability and folding of the EPPIN Kunitz domain, thus indirectly affecting sperm motility. Additional experiments will be required to determine whether the EPPIN WFDC domain acts as an intramolecular chaperone keeping the proper conformation of the Kunitz domain.

The reduced *in vitro* fertilizing ability of S21C- and Q20E-treated spermatozoa argues that blocking EPPIN's Kunitz and WFDC domains jeopardizes sperm traits essential for fertility. We emphasize that the 25–30% reduction in cleavage rates was observed using 4-fold lower antibody concentrations than those used in sperm motility assays. Owing to intrinsic limitations of the IVF protocol, we could not employ higher concentrations in our assay conditions. Additional concentration-response studies are warranted to show whether higher anti-EPPIN antibody concentrations can reduce fertilization rates further. Our findings suggest that EPPIN ligands targeting residues in both S21C and Q20E epitopes, such as the prototype compound EP055 (O'Rand *et al.*, 2018; Shan *et al.*, 2019), may effectively reduce fertilization, underscoring their potential clinical application as male contraceptive drugs. Indeed, our results may be translated to humans, given that the inhibition of human sperm motility parameters by EP055 (O'Rand *et al.*, 2018) may diminish their fertilizing ability *in vivo*.

It is known that capacitation-associated events rely on signaling pathways that lead to post-translational modifications of several sperm proteins (Visconti *et al.*, 1995b; Fraser, 2010; Battistone *et al.*, 2014). Among these post-translational modifications, tyrosine phosphorylation is an important event to trigger downstream signaling pathways that promote sperm capacitation (Visconti *et al.*, 1995b; Molina *et al.*, 2018). Activation of soluble adenylyl cyclase (ADCY10)/3′,5′-cyclic adenosine monophosphate (cAMP)/protein kinase A (PKA) pathway during sperm capacitation is crucial for capacitation-induced in tyrosine phosphorylation of sperm proteins (Visconti *et al.*, 1995b; Leclerc *et al.*, 1996). Antibodies mapping EPPIN C-terminus disturb cAMP production in human spermatozoa (O'Rand *et al.*, 2009), suggesting that downstream events, such as tyrosine phosphorylation, could be impaired. To address this hypothesis, we tested whether S21C and Q20E antibodies modify sperm capacitation-induced tyrosine phosphorylation. Our results ruled out this possibility since neither S21C nor Q20E antibodies changed the tyrosine phosphorylation profile during sperm capacitation *in vitro*. Intriguingly, EPPIN-binding partners SEMG1 and SVS2 inhibit capacitation-associated tyrosine phosphorylation in human and mouse spermatozoa, respectively (de Lamirande, 2007; Kawano and Yoshida, 2007). Thus, although their binding sites on EPPIN overlap with endogenous binding partners, the effects of S21C and Q20E antibodies on sperm capacitation are likely downstream of PKA-triggered protein phosphorylation, including disruption of intracellular Ca^{2+} increase or membrane hyperpolarization. Additional investigation will be required to test these hypotheses.

Novel pharmacological approaches for male contraception will represent an important step toward better gender equality in family planning. Taken together, we show that both WFDC and Kunitz domains of EPPIN play different roles in the control of progressive and hyperactivated mouse sperm motility, which leads to a decrease in their fertilizing ability. Our results underscore the rational design of EPPIN ligands simultaneously targeting residues within WFDC and Kunitz domains, which may provide a road for more potent spermostatic drugs with therapeutic applications in non-hormonal male contraception.

Supplementary data

Supplementary data are available at *Molecular Human Reproduction* online.

Data availability

The data underlying this article are available in the article and in its online supplementary material.

Acknowledgements

The authors are grateful to Luíz Antonio de Oliveira and Paulo Cesar Mioni for their technical assistance, Prof. Luiz Claudio Di Stasi, Ph.D., Prof. Rafael Henrique Nobrega, Ph.D. and Fernanda Franchi, Ph.D. for their help in immunofluorescence experiments; Alexandre D. Andrade, M.Sc. and Joel Gabrili, M.Sc., for their assistance in animal experiments and cell fractionation experiments; and Guillermina Luque, Ph.D. and Martina Jabloñski, M.Sc., for their help in sperm capacitation and IVF studies. The authors also thank Prof. Pablo Visconti for providing the protocols for cell fractionation and Prof. Michael O'Rand and Katherine Hamil, M.Sc., for reading the article.

Authors' roles

E.J.R.S conceived, designed the research, wrote the article and prepared the figures. A.A.S.S., T.R.F.R., N.A.P.M., H.K. and M.T.M. performed the experiments. M.C.W.A., M.T.M, F.F.P.-L. and M.G.B. contributed to experimental design and data analysis. E.J.R.S., T.R.F.R., M.T.M. and A.A.S.S. performed data analysis. All authors reviewed the article.

Funding

This study was funded by São Paulo Research Foundation (FAPESP, grant numbers 2015/08227-0, 2017/11363-8, and 2019/13661-1), Coordenação de Aperfeiçoamento de Pessoal de Nível Superior (CAPES, financial code 001) and Conselho Nacional de Desenvolvimento Científico e Tecnológico (CNPq). This work was also supported by *Agencia Nacional de Promoción Científica y Tecnológica* (PICT 2017-3047 to M.G.B.).

Conflict of interest

The authors declare that they have no conflict of interest.

References

Alquézar-Baeta C, Gimeno-Martos S, Miguel-Jiménez S, Santolaria P, Yániz J, Palacín I, Casao A, Cebrián-Pérez JÁ, Muiño-Blanco T, Pérez-Pé R. OpenCASA: a new open-source and scalable tool for sperm quality analysis. *PLoS Comput Biol* 2019;**15**:e1006691.

Alvau A, Battistone MA, Gervasi MG, Navarrete FA, Xu X, Sánchez-Cárdenas C, De la Vega-Beltran JL, Da Ros VG, Greer PA, Darszon A *et al*. The tyrosine kinase FER is responsible for the capacitation-associated increase in tyrosine phosphorylation in murine sperm. *Development* 2016;**143**:2325–2333.

Amory JK. Male contraception. *Fertil Steril* 2016;**106**:1303–1309.

Battistone MA, Alvau A, Salicioni AM, Visconti PE, Da Ros VG, Cuasnicú PS. Evidence for the involvement of proline-rich tyrosine kinase 2 in tyrosine phosphorylation downstream of protein kinase A activation during human sperm capacitation. *Mol Hum Reprod* 2014;**20**:1054–1066.

Cancel AM, Lobdell D, Mendola P, Perreault SD. Objective evaluation of hyperactivated motility in rat spermatozoa using computer-assisted sperm analysis. *Hum Reprod* 2000;**15**:1322–1328.

Carlson AE, Westenbroek RE, Quill T, Ren D, Clapham DE, Hille B, Garbers DL, Babcock DF. CatSper1 required for evoked Ca2+ entry and control of flagellar function in sperm. *Proc Natl Acad Sci U S A* 2003;**100**:14864–14868.

Chen Z, He W, Liang Z, Yan P, He H, Tang Y, Zhang J, Shen Z, Ni B, Wu Y *et al*. Protein prime-peptide boost as a new strategy induced an Eppin dominant B-cell epitope specific immune response and suppressed fertility. *Vaccine* 2009;**27**:733–740.

Clauss A, Lilja H, Lundwall A. The evolution of a genetic locus encoding small serine proteinase inhibitors. *Biochem Biophys Res Commun* 2005;**333**:383–389.

de Lamirande E. Semenogelin, the main protein of the human semen coagulum, regulates sperm function. *Semin Thromb Hemost* 2007;**33**:60–68.

de Lamirande E, Lamothe G. Levels of semenogelin in human spermatozoa decrease during capacitation: involvement of reactive oxygen species and zinc. *Hum Reprod* 2010;**25**:1619–1630.

de Lamirande E, Yoshida K, Yoshiike TM, Iwamoto T, Gagnon C. Semenogelin, the main protein of semen coagulum, inhibits human sperm capacitation by interfering with the superoxide anion generated during this process. *J Androl* 2001;**22**:672–679.

Ding X, Zhang J, Bian Z, Xia Y, Lu C, Gu A, Li Y, Song L, Wang S, Wang X. Variants in the Eppin gene show association with semen quality in Han-Chinese population. *Reprod Biomed Online* 2010a;**20**:125–131.

Ding X, Zhang J, Fei J, Bian Z, Li Y, Xia Y, Lu C, Song L, Wang S, Wang X. Variants of the EPPIN gene affect the risk of idiopathic male infertility in the Han-Chinese population. *Hum Reprod* 2010b;**25**:1657–1665.

Drevet JR. Epididymal approaches to male contraception. *Basic Clin Androl* 2018;**28**:12.

Ernesto JI, Weigel Muñoz M, Battistone MA, Vasen G, Martínez-López P, Orta G, Figueiras-Fierro D, De la Vega-Beltran JL, Moreno IA, Guidobaldi HA *et al*. CRISP1 as a novel CatSper regulator that modulates sperm motility and orientation during fertilization. *J Cell Biol* 2015;**210**:1213–1224.

Fraser LR. The "switching on" of mammalian spermatozoa: Molecular events involved in promotion and regulation of capacitation. *Mol Reprod Dev* 2010;**77**:197–208.

Freitas MJ, Vijayaraghavan S, Fardilha M. Signaling mechanisms in mammalian sperm motility. *Biol Reprod* 2017;**96**:2–12.

Goodson SG, Zhang Z, Tsuruta JK, Wang W, O'Brien DA. Classification of mouse sperm motility patterns using an automated multiclass support vector machines model. *Biol Reprod* 2011;**84**:1207–1215.

Gossett DR, Kiley JW, Hammond C. Contraception is a fundamental primary care service. *JAMA* 2013;**309**:1997–1998.

Ho HC, Suarez SS. Hyperactivation of mammalian spermatozoa: function and regulation. *Reproduction* 2001;**122**:519–526.

Jamur MC, Oliver C. Permeabilization of cell membranes. *Methods Mol Biol* 2010;**588**:63–66.

Kawano N, Araki N, Yoshida K, Hibino T, Ohnami N, Makino M, Kanai S, Hasuwa H, Yoshida M, Miyado K *et al*. Seminal vesicle protein SVS2 is required for sperm survival in the uterus. *Proc Natl Acad Sci U S A* 2014;**111**:4145–4150.

Kawano N, Yoshida M. Semen-coagulating protein, SVS2, in mouse seminal plasma controls sperm fertility. *Biol Reprod* 2007;**76**:353–361.

Leclerc P, de Lamirande E, Gagnon C. Cyclic adenosine 3',5'monophosphate-dependent regulation of protein tyrosine phosphorylation in relation to human sperm capacitation and motility. *Biol Reprod* 1996;**55**:684–692.

Long JE, Lee MS, Blithe DL. Male contraceptive development: update on novel hormonal and nonhormonal methods. *Clin Chem* 2019;**65**:153–160.

Mariani NAP, Camara AC, Silva AAS, Raimundo TRF, Andrade JJ, Andrade AD, Rossini BC, Marino CL, Kushima H, Santos LD *et al*. Epididymal protease inhibitor (EPPIN) is a protein hub for seminal

vesicle-secreted protein SVS2 binding in mouse spermatozoa. *Mol Cell Endocrinol* 2020;**506**:110754.

McCrudden MT, Dafforn TR, Houston DF, Turkington PT, Timson DJ. Functional domains of the human epididymal protease inhibitor, eppin. *FEBS J* 2008;**275**:1742–1750.

Mitra A, Richardson RT, O'Rand MG. Analysis of recombinant human semenogelin as an inhibitor of human sperm motility. *Biol Reprod* 2010;**82**:489–496.

O'Rand MG, Silva EJR, Hamil KG. Non-hormonal male contraception: a review and development of an Eppin based contraceptive. *Pharmacol Ther* 2016;**157**:105–111.

O'Rand MG, Widgren EE. Loss of calcium in human spermatozoa via EPPIN, the semenogelin receptor. *Biol Reprod* 2012;**86**:55–57.

O'Rand MG, Widgren EE, Beyler S, Richardson RT. Inhibition of human sperm motility by contraceptive anti-Eppin antibodies from infertile male monkeys: effect on cyclic adenosine monophosphate. *Biol Reprod* 2009;**80**:279–285.

O'Rand MG, Widgren EE, Hamil KG, Silva EJ, Richardson RT. Epididymal protein targets: a brief history of the development of epididymal protease inhibitor as a contraceptive. *J Androl* 2011;**32**:698–704.

O'Rand MG, Widgren EE, Sivashanmugam P, Richardson RT, Hall SH, French FS, VandeVoort CA, Ramachandra SG, Ramesh V, Jagannadha Rao A. Reversible immunocontraception in male monkeys immunized with Eppin. *Science* 2004;**306**:1189–1190.

O'Rand MG, Hamil KG, Adevai T, Zelinski M. Inhibition of sperm motility in male macaques with EP055, a potential non-hormonal male contraceptive. *PLoS One* 2018;**13**:e0195953.

Molina P, Luque LC, Balestrini GM, Marín-Briggiler PA, Romarowski CI, Buffone A, Molecular MG. Basis of human sperm capacitation. *Front Cell Dev Biol* 2018;**6**:72.

Richardson RT, Sivashanmugam P, Hall SH, Hamil KG, Moore PA, Ruben SM, French FS, O'Rand M. Cloning and sequencing of human Eppin: a novel family of protease inhibitors expressed in the epididymis and testis. *Gene* 2001;**270**:93–102.

Robertson MJ, Kent K, Tharp N, Nozawa K, Dean L, Mathew M, Grimm SL, Yu Z, Légaré C, Fujihara Y *et al*. Large-scale discovery of male reproductive tract-specific genes through analysis of RNA-seq datasets. *BMC Biol* 2020;**18**:103.

Rueden CT, Schindelin J, Hiner MC, DeZonia BE, Walter AE, Arena ET, Eliceiri KW. ImageJ2: ImageJ for the next generation of scientific image data. *BMC Bioinformatics* 2017;**18**:529.

Sakaguchi D, Miyado K, Iwamoto T, Okada H, Yoshida K, Kang W, Suzuki M, Yoshida M, Kawano N. Human semenogelin I promotes sperm survival in the mouse female reproductive tract. *Int J Mol Sci* 2020;**21**:3961.

Sedgh G, Singh S, Hussain R. Intended and unintended pregnancies worldwide in 2012 and recent trends. *Stud Fam Plann* 2014;**45**:301–314.

Shan C, Li H, Zhang Y, Li Y, Chen Y, He W. Binding interactions of epididymal protease inhibitor and semenogelin-1: a homology modeling, docking and molecular dynamics simulation study. *PeerJ* 2019;**7**:e7329.

Silva EJR, Hamil KG, O'Rand MG. Interacting proteins on human spermatozoa: adaptive evolution of the binding of semenogelin I to EPPIN. *PLoS One* 2013;**8**:e82014.

Silva EJR, Hamil KG, Richardson RT, O'Rand MG. Characterization of EPPIN's semenogelin I binding site: a contraceptive drug target. *Biol Reprod* 2012a;**87**:56–58.

Silva EJR, Patrão MTCC, Tsuruta JK, O'Rand MG, Avellar MCW. Epididymal protease inhibitor (EPPIN) is differentially expressed in the male rat reproductive tract and immunolocalized in maturing spermatozoa. *Mol Reprod Dev* 2012b;**79**:832–842.

Sivashanmugam P, Hall SH, Hamil KG, French FS, O'Rand MG, Richardson RT. Characterization of mouse Eppin and a gene cluster of similar protease inhibitors on mouse chromosome 2. *Gene* 2003;**312**:125–134.

Suarez SS. Control of hyperactivation in sperm. *Hum Reprod Update* 2008;**14**:647–657.

Summers MC, McGinnis LK, Lawitts JA, Raffin M, Biggers JD. IVF of mouse ova in a simplex optimized medium supplemented with amino acids. *Hum Reprod* 2000;**15**:1791–1801.

Sun L-L, Li J-T, Wu Y-Z, Ni B, Long L, Xiang Y-L, He W, Liang Z-Q. Screening and identification of dominant functional fragments of human epididymal protease inhibitor. *Vaccine* 2010;**28**:1847–1853.

Tsui AO, McDonald-Mosley R, Burke AE. Family planning and the burden of unintended pregnancies. *Epidemiol Rev* 2010;**32**:152–174.

Turner RM. Moving to the beat: a review of mammalian sperm motility regulation. *Reprod Fertil Dev* 2006;**18**:25–38.

Visconti PE, Bailey JL, Moore GD, Pan D, Olds-Clarke P, Kopf GS. Capacitation of mouse spermatozoa. I. Correlation between the capacitation state and protein tyrosine phosphorylation. Development 1995a;**121**:1129–1137.

Visconti PE, Moore GD, Bailey JL, Leclerc P, Connors SA, Pan D, Olds-Clarke P, Kopf GS. Capacitation of mouse spermatozoa. II. Protein tyrosine phosphorylation and capacitation are regulated by a cAMP-dependent pathway. *Development* 1995b;**121**:1139–1150.

Visconti PE, Olds-Clarke P, Moss SB, Kalab P, Travis AJ, De Las Heras M, Kopf GS. Properties and localization of a tyrosine phosphorylated form of hexokinase in mouse sperm. *Mol Reprod Dev* 1996;**43**:82–93.

Wang Z, Widgren EE, Richardson RT, O'Rand MG. Characterization of an Eppin Protein Complex from Human Semen and Spermatozoa. *Biol Reprod* 2007a;**77**:476–484.

Wang Z, Widgren EE, Richardson RT, Orand MG. Eppin: a molecular strategy for male contraception. *Soc Reprod Fertil Suppl* 2007b;**65**:535–542.

Wang Z, Widgren EE, Sivashanmugam P, O'Rand MG, Richardson RT. Association of eppin with semenogelin on human spermatozoa. *Biol Reprod* 2005;**72**:1064–1070.

Yenugu S, Richardson RT, Sivashanmugam P, Wang Z, O'Rand MG, French FS, Hall SH. Antimicrobial activity of human EPPIN, an androgen-regulated, sperm-bound protein with a whey acidic protein motif. *Biol Reprod* 2004;**71**:1484–1490.

Zar JH. *Biostatistical Analysis*. 5th edn, 2010. Pearson Prentice Hall, New Jersey, NJ, USA.